

Synthesis, structures, and photoluminescence properties of three metal(II) coordination polymers derived from a flexible tripodal ligand and 2,6-pyridinedicarboxylic acid

Shi-Meng Wang · Ling Qian · Hong-Ye Bai ·
Wei-Qiang Fan · Chun-Bo Liu · Guang-Bo Che

Received: 10 October 2012 / Accepted: 6 November 2012 / Published online: 22 November 2012
© Springer Science+Business Media Dordrecht 2012

Abstract Using a flexible tripodal ligand N,N',N'' -tris(3-pyridyl)-1,3,5-benzenetricarboxamide and 2,6-pyridinedicarboxylic acid, three metal(II) complexes formulated as $[\text{Co}(\text{pydc})(\text{L})_n]$ (**1**), $[\text{Zn}(\text{pydc})(\text{L})_n]$ (**2**), $\{[\text{Ni}(\text{pydc})(\text{L})] \cdot 2\text{H}_2\text{O}\}_n$ (**3**) ($\text{L} = N,N',N''$ -tris(3-pyridyl)-1,3,5-benzenetricarboxamide, $\text{H}_2\text{pydc} = 2,6$ -pyridinedicarboxylic acid) have been hydrothermally synthesized and structurally characterized by physico-chemical and spectroscopic methods and single-crystal diffraction. In compounds **1** and **2**, the L ligands acts as bridges to link the metal atoms into zigzag chain structures, which are further extended into three-dimensional (3D) metal–organic supramolecular frameworks by hydrogen bond interactions. In compound **3**, the L ligands link three Ni(II) centers to form a two-dimensional (2D) hcb layered structure, and then, the adjacent nets interweave in parallel to generate a 3D structure by $2\text{D} \rightarrow 3\text{D}$ interpenetration. The thermal stabilities of **1–3** and the luminescent properties of **2** in the solid state are also discussed.

Keywords Coordination polymers · Flexible ligands · Luminescence

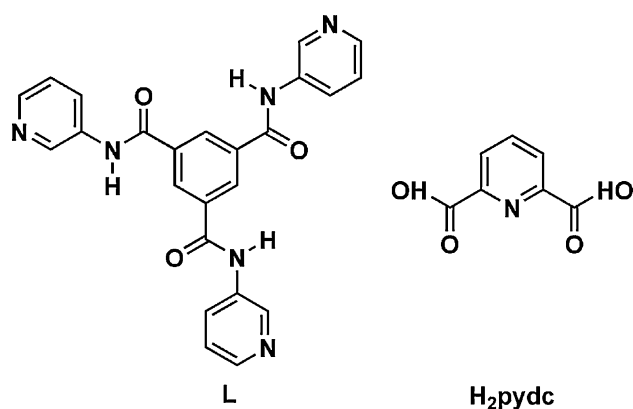
Introduction

Coordination frameworks with transition metal atoms and organic bridging ligands have been rapidly developed in recent years and attracted great interest from chemists, not only due to their intriguing topologies, such as molecular cage, honeycomb, grid, ladder, rotaxane, catenane, but also due to their interesting properties and potential applications, such as ion exchange, gas storage, recognition, magnetism [1–6]. However, it is still a big challenge to predict the exact structures of coordination polymers with desired properties because many factors affect the result, such as the coordination geometry of the central metal atoms, connection modes of organic ligands, reaction temperature, the ratio of solvents, pH value, and so on [7–10]. The most effective approach to overcome this problem is the appropriate choice of well-designed organic bridging ligands, together with the metal centers with various coordination preferences [11–13].

Up to now, flexible tripodal ligands provide one such option and have drawn much attention. The flexible aryl-heterocyclic tripodal ligands, such as 1,3,5-tris(imidazol-1-ylmethyl)benzene, 1,3,5-tris(imidazol-1-ylmethyl)-2,4,6-trimethylbenzene, 1,3,5-tris(4-pyridylmethyl)benzene, 1,3,5-tris(pyrazol-1-ylmethyl)-2,4,6-triethylbenzene, and 1,3,5-tris[(ben-zimidazol-1-yl)methyl]-2,4,6-trimethylbenzene [14–17], have proved to be useful building blocks to generate interesting metal complexes. In contrast to the rigid tripodal ligands with little or no conformational changes when they interact with metal salts, the flexible tripodal ligands have much more abundant possible conformations and coordination modes than the rigid ones due to their flexibility; thus, they can adopt different conformations according to the different geometric requirements of the metal atoms and may offer various possibilities for syntheses

Electronic supplementary material The online version of this article (doi:10.1007/s11243-012-9673-5) contains supplementary material, which is available to authorized users.

S.-M. Wang · L. Qian · H.-Y. Bai · W.-Q. Fan · C.-B. Liu ·
G.-B. Che (✉)
School of Chemistry and Chemical Engineering, Jiangsu
University, Zhenjiang 212013, People's Republic of China
e-mail: bhy19841009@yahoo.com.cn;
guangbocheujs@yahoo.com.cn



Scheme 1 Ligands used in this work

of intriguing MOFs with diverse structures and useful properties [18–20]. In addition, polycarboxylate organic groups have been found to be excellent structural contributors for their various coordination modes. Carboxylate groups can act not only as hydrogen bond acceptors but also as hydrogen bond donors, which would enrich the versatility of coordination complexes [20–22]. On the basis of the above considerations, we chose *N,N',N''*-tris(3-pyridyl)-1,3,5-benzenetricarboxamide (L) and 2,6-pyridinedicarboxylic acid (H_2pydc) as functional ligands. In this work, a series of coordination compounds $[Co(pydc)(L)]_n$ (**1**), $[Zn(pydc)(L)]_n$ (**2**), $\{[Ni(pydc)(L)] \cdot 2H_2O\}_n$ (**3**) ($L = N,N',N''$ -tris(3-pyridyl)-1,3,5-benzenetricarboxamide, $H_2pydc = 2,6$ -pyridinedicarboxylic acid) were prepared by the hydrothermal method (Scheme 1). The thermal stabilities of complexes **1–3** and fluorescent properties of complex **2** have been investigated in the solid state at room temperature.

Experimental section

Materials and physical measurements

The L ligand was prepared according to the literature [23]. All other chemicals were of reagent grade and purchased from Alfa Aesar without further purification. Elemental analyses were performed with a Perkin-Elmer 240C element analyzer. IR spectra were recorded as KBr pellets in the range 4,000–400 cm^{-1} on Perkin-Elmer spectrometer. Powder X-ray diffraction patterns (PXRD) were recorded on a Bruker D8 Advance diffractometer with Cu-K α radiation ($\lambda = 1.54178 \text{ \AA}$) ranging from 5° to 35°. Thermogravimetric analysis (TGA) was performed on a NET-ZCH STA 449C with a heating rate of 10 $^{\circ}C \text{ min}^{-1}$ under air atmosphere. The photoluminescent properties of the ligands and compounds were measured on a Perkin-Elmer LS 55 luminescence spectrometer.

Synthesis of $[Co(pydc)(L)]_n$ (**1**)

A mixture of $CoCO_3$ (0.0090 g, 0.075 mmol), H_2pydc (0.0125 g, 0.075 mmol), L (0.0219 g, 0.05 mmol), and water (10 mL) was stirred and then heated at 120 $^{\circ}C$ in a Teflon-lined autoclave for 3 days, followed by slow cooling to room temperature. The resulting purple prismatic crystals were collected, washed with water, and dried in air (yield, ca. 37 % based on Co). Elemental anal. found: C, 57.25; H, 3.24; N, 13.81 %. Calcd for $C_{31}H_{21}CoN_7O_7$ (Mr = 662.48): C, 56.20; H, 3.19; N, 14.80 %. IR (cm^{-1}): 3242 (w), 3072 (w), 1671 (s), 1635 (s), 1550 (s), 1478 (s), 1417 (w), 1357 (m), 1309 (m), 1236 (m), 1067 (m), 1062 (s), 910 (w), 813 (s), 717 (s), 656 (m), 584 (w), 427 (w).

Synthesis of $[Zn(pydc)(L)]_n$ (**2**)

A mixture of $ZnCO_3$ (0.0125 g, 0.1 mmol), H_2pydc (0.0167 g, 0.1 mmol), L (0.0219 g, 0.05 mmol), and water (10 mL) was stirred and then heated at 150 $^{\circ}C$ in a Teflon-lined autoclave for 3 days, followed by slow cooling to room temperature. The resulting colorless prismatic crystals were collected. The yield of the colorless prismatic crystals is ca. 45 % based on Zn. Elemental anal. found: C, 56.37; H, 3.82; N, 14.81 %. Calcd for $C_{31}H_{21}ZnN_7O_7$ (Mr = 668.92): C, 55.69; H, 3.16; N, 14.66 %. IR (cm^{-1}): 3258 (m), 3070 (w), 1681 (s), 1639 (s), 1544 (s), 1474 (s), 1424 (w), 1373 (m), 1301 (m), 1257 (m), 1064 (m), 1047 (s), 927 (w), 807 (s), 739 (s), 653 (m), 585 (w), 396 (w).

Synthesis of $\{[Ni(pydc)(L)] \cdot 2H_2O\}_n$ (**3**)

The synthesis of complex **3** was carried out as described above for complex **1** except that $NiCO_3$ was used instead of $CoCO_3$. The resulting green prismatic crystals were collected. The yield of the green prismatic crystals is ca. 48 % based on Ni. Elemental anal. found: C, 54.25; H, 4.10; N, 15.21 %. Calcd for $C_{31}H_{23}NiN_7O_9$ (Mr = 696.27): C, 53.48; H, 3.33; N, 14.08 %. IR (cm^{-1}): 3233 (w), 3065 (w), 1660 (s), 1629 (s), 1538 (s), 1492 (s), 1415 (w), 1355 (m), 1294 (m), 1248 (m), 1086 (m), 1080 (s), 912 (w), 805 (s), 698 (s), 658 (m), 591 (w), 438 (w).

Crystal structure determination

Single-crystal X-ray diffraction data of the three complexes were recorded on an Oxford Diffraction Gemini R Ultra diffractometer with graphite-monochromated Mo-K α radiation ($\lambda = 0.71073 \text{ \AA}$) at 293 K. All non-hydrogen atoms were refined anisotropically, and the hydrogen atoms of carbon atoms were generated geometrically. The hydrogen atoms of water molecules were located from difference Fourier map except OW2 in compound **3**. The

Table 1 Crystal data and structure refinement for complexes **1–3**

Compounds	1	2	3
Formula	C ₃₁ H ₂₁ CoN ₇ O ₇	C ₃₁ H ₂₁ ZnN ₇ O ₇	C ₃₁ H ₂₅ NiN ₇ O ₉
fw	662.48	668.92	698.29
Crystal system	Monoclinic	Monoclinic	Hexagonal
Spacegroup	P2 ₁ /n	P2 ₁ /n	R3c
<i>a</i> (Å)	13.875(2)	14.192(6)	27.864(5)
<i>b</i> (Å)	9.366(1)	9.030(4)	27.864(5)
<i>c</i> (Å)	21.546(3)	22.118(9)	20.187(5)
α (°)	90	90	90
β (°)	98.227(2)	100.322(5)	90
γ (°)	90	90	120
<i>V</i> (Å ³)	2771.1(6)	2788.5(19)	13573(5)
<i>Z</i>	4	4	18
<i>D</i> _{calcd} (g cm ⁻³)	1.588	1.593	1.538
<i>F</i> (000)	1356	1368	6480
θ (°)	1.64–27.56	1.59–27.98	1.46–27.51
μ (mm ⁻¹)	0.685	0.946	0.712
GOF on <i>F</i> ²	1.061	1.022	1.020
<i>R</i> ₁ ^a [<i>I</i> >2 σ (<i>I</i>)]	0.0426	0.0424	0.0409
<i>wR</i> ₂ ^b [<i>I</i> >2 σ (<i>I</i>)]	0.1150	0.0891	0.0900

hydrogen atoms bonded to nitrogen atoms were also located in a difference map and refined freely. All the structures were solved by Direct Methods of SHELXS-97 and refined by full-matrix least-squares techniques using the SHELXL-97 program [24]. The hydrogen atoms were assigned with common isotropic displacement factors. Crystallographic data and structure processing parameters for complexes **1–3** are summarized in Table 1. Selected bond distances and angles and hydrogen bonds for them are listed in Table S1a–S3b (Supporting Information).

The experimental PXRD patterns of the polymers are similar to those calculated from their single-crystal X-ray data, which are a good indication of phase purity of the products (Fig. S1). The differences in intensity between the experimental and simulated XRPD patterns may be due to the preferred orientation of the powder samples during the experiment.

Results and discussion

Crystal structure of [Co(pydc)(L)]_n (**1**)

Complex **1** crystallizes in monoclinic space group P2₁/n. The X-ray crystallographic study shows that the asymmetric unit of complex **1** consists of one Co(II) atom, one pydc ligand, and one L ligand (Fig. 1a). The Co(II) center is five-coordinated by three nitrogen atoms from two L ligands and one pydc ligand, and two oxygen atoms from

one pydc ligand, showing a tetragonal pyramidal coordination geometry. The Co–O bond distances are 2.075(2) and 2.149(2) Å, respectively, and the Co–N bond lengths in the range of 2.002(2)–2.129(2) Å. Each ligand L acts as a bidentate ligand binding with two Co atoms in Mode I (Scheme 2), forming a 1D infinite zigzag chain (Fig. 1b). The adjacent 1D infinite chains are connected by one kind of hydrogen bonding interactions between the oxygen atom of pydc ligands and nitrogen atom of L ligand [N5...O4 3.145(3) Å] to form a 2D supramolecular network parallel to the *ab* plane (Fig. 1c). The adjacent 2D supramolecular layers are further connected by two other kinds of hydrogen bonding interactions [N3...O2 2.840(3) Å, 162(3)° and N6...O(5) 2.943(3) Å, 168(3)°, respectively] to form a three-dimensional (3D) supramolecular network (Fig. 1d, Table S1b). Additionally, the supramolecular network is further stabilized by two types of π – π stacking interactions. One exists between the phenyl rings of L ligands with the centroid-to-centroid separation of 3.565 Å, and the other appears between the phenyl ring of L ligand and pyridine ring of pydc ligand with a centroid-to-centroid distance of 3.8991 Å.

Crystal structure of [Zn(pydc)(L)]_n (**2**)

When CoCO₃ was replaced by ZnCO₃, a 3D supramolecular network **2** was obtained. Complex **2** is isomorphous with **1**. The X-ray crystallographic study shows that there are one Zn(II) atom, one pydc ligand, and one L ligand in the asymmetric unit of complex **2** (Fig. 2a). Similar to compound **1**, the structural stability of compound **2** is also provided by hydrogen bonding interactions between the N atom of the L and O atoms of the pydc (N4...O4 = 3.238(3) Å and N5...O2 = 2.859(3) Å, respectively) and between the N atom of the one kind of L and another kind of L (N3...O7 = 2.980(3) Å). In addition, the crystal structure of complex **2** is further strengthened through the π – π stacking interactions between the phenyl rings of ligand L, with the centroid-to-centroid separation of 3.579 Å.

Crystal structure of {[Ni(pydc)(L)]·2H₂O}_n (**3**)

When NiCO₃ was selected to react with pydc and L under similar synthetic conditions, a structurally different complex **3** was obtained. As shown in Fig. 3a, the structure of **3** consists of one crystallographically independent Ni(II) atom, one pydc ligand, one L ligand, and two lattice water molecules. The Ni(II) atom is in an distorted octahedral NiN₄O₂ coordination geometry, coordinated by three nitrogen atoms from three L ligands (Ni–N 2.094(3)–2.143(3) Å) and one nitrogen atom from one pydc ligand (Ni–N 2.005(4) Å) in the equatorial positions and two carboxylate oxygen atoms from one pydc ligand (Ni–O

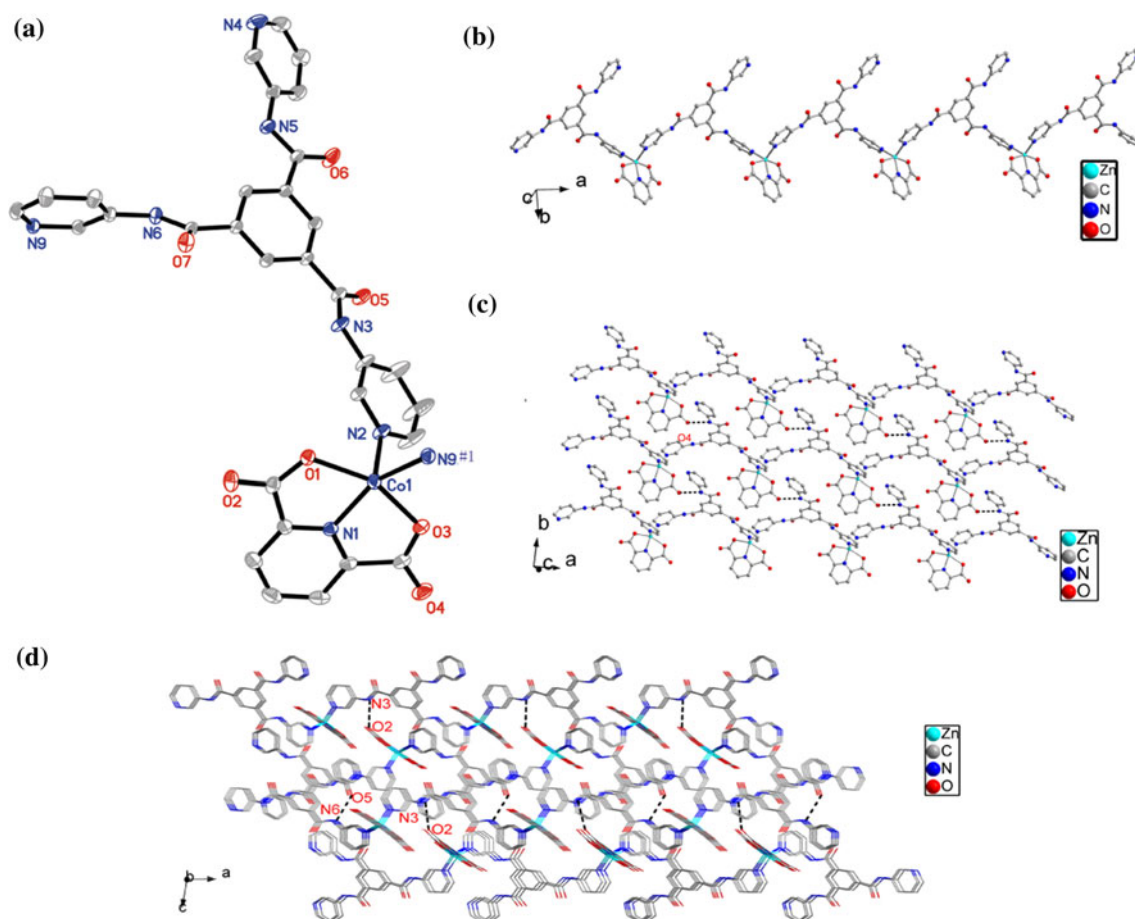
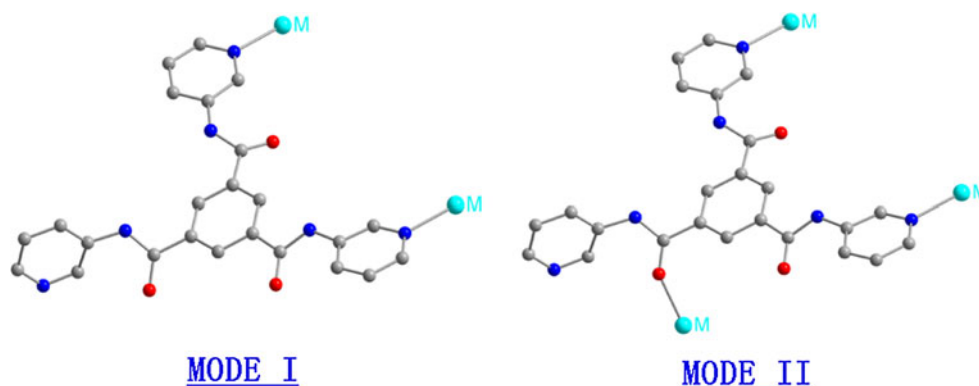


Fig. 1 **a** Coordination environment around the Co(II) centers in **1**. Hydrogen atoms are omitted for clarity. Symmetry code: #1 = $x - 1, y, z$; #2 = $x + 1, y, z$; **b** the 1D structure of complex **1**; **c** the 2D layer

of **1** formed between 1D chains by hydrogen bonding interactions; **d** the 3D supramolecular structure of **1** formed through hydrogen bonding interactions

Scheme 2 The coordination modes of the L ligand



2.078(3) and 2.231(2) Å, respectively) in the apical positions. Each L ligand coordinates to three Ni(II) atoms (Mode II) to form a two-dimensional (2D) layer structure parallel to the ab plane (Fig. 3b). Topological analysis of this compound reveals that it is a 3-connected net with hcb topology, if the Ni(II) atoms are regarded as linkers, and ligands L are considered as 3-connected nodes (Fig. 3c). Adjacent nets interweave in parallel to generate a 3D

structure (2D \rightarrow 3D parallel) (Fig. 3d). The crystal structure of complex **3** is further strengthened through hydrogen bonding interactions and π - π stacking interactions.

Coordination modes of ligand L

The L ligand can bend and rotate freely when coordinating to the central metals due to the flexible nature of the three

amide groups between the three pyridine rings [25–27]. It can take on rich coordination modes, which may greatly extend and enrich the MOFs' structures. Scheme 2 shows two different coordination modes of L ligands observed in complexes 1–3, that is, tridentate mode and bidentate

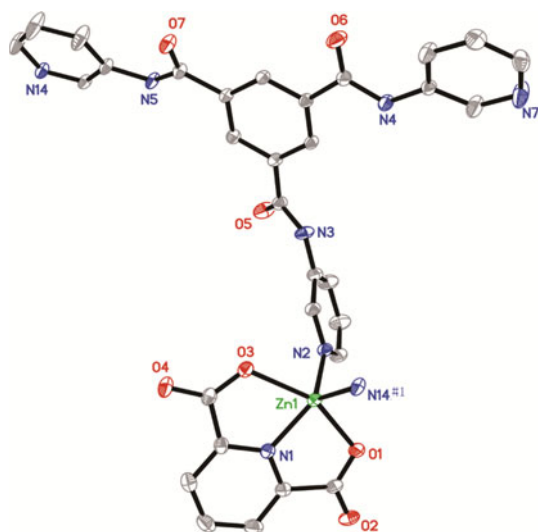


Fig. 2 ORTEP view of **2** showing the local coordination environment of Zn(II) atom with hydrogen atoms for clarity. Symmetry code: #1 = $x - 1, y, z$; #2 = $x + 1, y, z$

mode, respectively. L molecules adopting the Mode I coordination link two M (M = Co (**1**), Zn (**2**)) atoms to construct one-dimensional (1D) structures in **1** and **2**. Moreover, the adjacent 1D infinite chains are connected by hydrogen bonding interactions to form a 3D supramolecular network. For complex **3**, the L ligands act as tridentate ligands (Mode II) to link three metal atoms through pyridyl nitrogen atoms and carbonyl oxygen atom. In fact, ligand L has six potential coordination nodes (three pyridyl nitrogen atoms and three carbonyl oxygen atoms), which can coordinate to metal atoms entirely or partly and result in many possible coordination modes. The L ligand may act as several kinds of polydentate ligand (from monodentate to hexadentate). Thus, it is a very useful ligand to construct interesting MOF structures in the future work.

Thermal analyses

In order to characterize the compounds more fully in terms of thermal stability, their thermal behaviors were studied by TGA. For compound **1**, the decomposition of the compound occurs at 416 °C, indicating high thermal stability of the frameworks. For compound **2**, only one step occurs from 412 to 491 °C corresponding to the decomposition of the coordination framework with ZnO as the

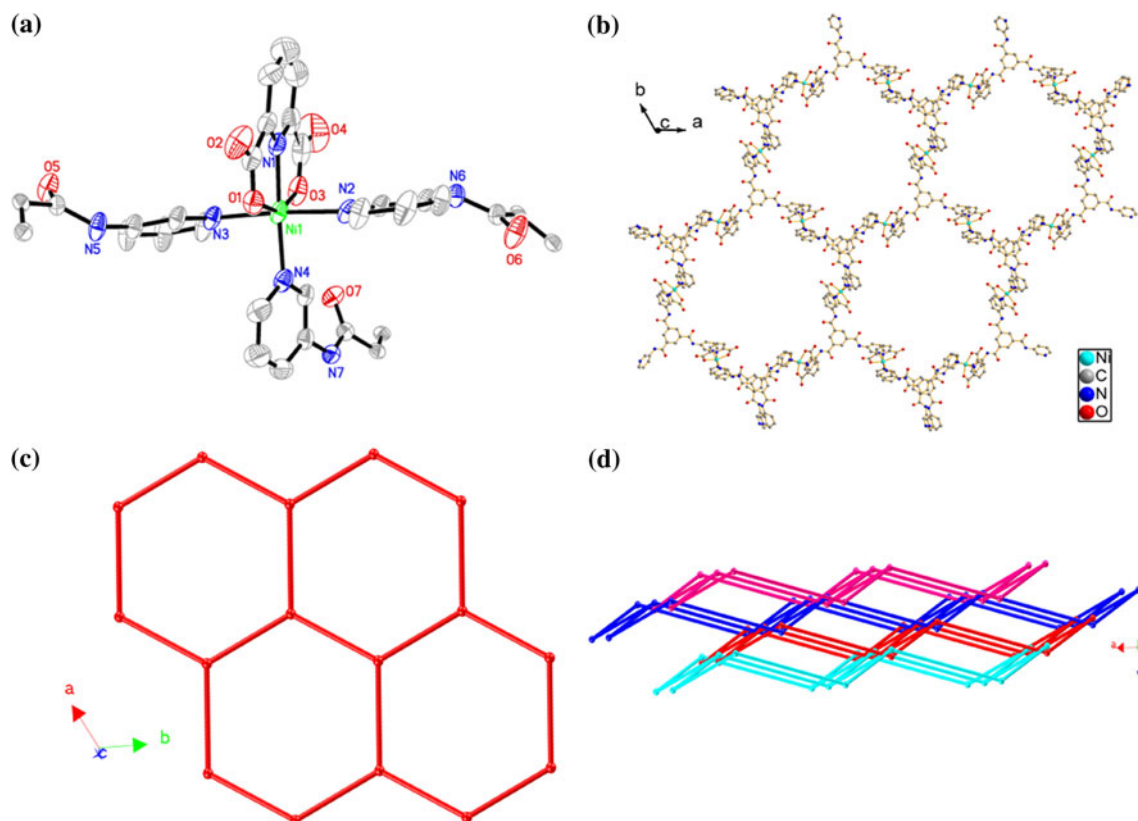


Fig. 3 **a** Coordination environment around the Ni(II) centers in **3**. Hydrogen atoms and solvent molecules are omitted for clarity; **b** the 2D bilayer structure; **c** schematic diagram of the 2D net in **3**; **d** schematic view of the 2D → 3D interpenetrated framework of complex **3**

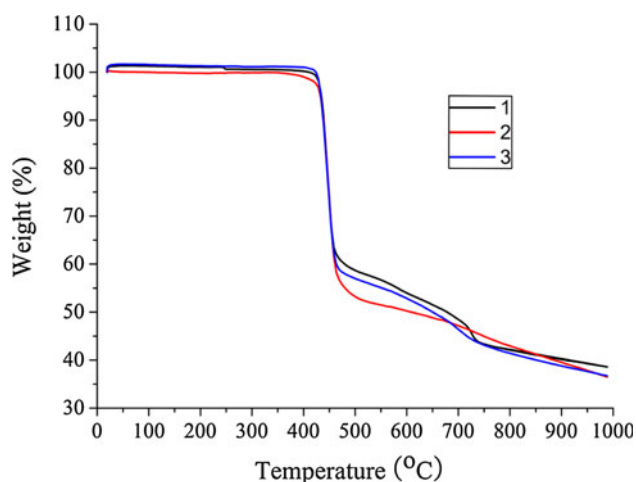


Fig. 4 TGA curves of compounds 1–3

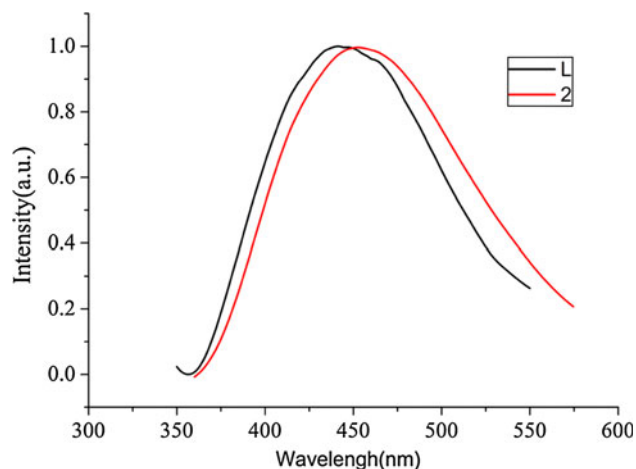


Fig. 5 Solid-state photoluminescent spectra of L and compound 2 at room temperature

residue (obsd 12.59 %, calcd 12.23 %). For compound 3, the weight loss in the range from room temperature to 239 °C corresponds to the departure of water molecules (obsd 5.32 %, calcd 5.17 %). The anhydrous compound begins to decompose at 417 °C (Fig. 4).

Luminescent properties

Coordination polymers, especially those with d^{10} metal centers, have been investigated for their luminescent properties and potential applications. Hence, the luminescent properties of compound 2 and free ligand L were measured in the solid state, as shown in Fig. 5. The maximum of the emission band is observed at 441 nm ($\lambda_{\text{ex}} = 335$ nm) for free L, which is ascribed to the $\pi^* \rightarrow n$ or $\pi^* \rightarrow \pi$ electronic transition of the free ligand [28, 29]. For compound 2, its peak is at 453 nm ($\lambda_{\text{ex}} = 345$ nm). Since the profiles and locations of the

emission band in the spectra of the compounds are similar to those observed in the free ligand, they can be assigned mainly to intraligand transitions.

Conclusions

In this work, three metal(II) coordination polymers based on *N,N',N''*-tris(3-pyridyl)-1,3,5-benzenetricarboxamide and 2,6-pyridinedicarboxylic acid have been successfully prepared under hydrothermal conditions. Compounds 1 and 2 are infinite 1D zigzag chain structures, whereas compound 3 possesses a 2D \rightarrow 3D interpenetration structure based on the hcb net. It is anticipated that more metal complexes containing polydentate neutral ligands with interesting structures as well as physical properties will be synthesized.

Supporting information

Selected bond distances and angles, and hydrogen bonding geometry for compounds 1–3. CCDC 898448–898450 contain the supplementary crystallographic data for 1–3. These data can be obtained free of charge via <http://www.ccdc.cam.ac.uk/conts/retrieving.html> or from the Cambridge Crystallographic Data Centre, 12 Union Road, Cambridge CB2 1EZ, UK; fax: (+44) 1223-336-033; or e-mail: deposit@ccdc.cam.ac.uk.

Acknowledgments The authors are grateful for the National Natural Science Foundation of China (Grant No. 21201085), Natural Science Foundation of Jiangsu Province (SBK2011460), Start-Up Foundation of Jiangsu University (11JDG105, 11JDG153, 11JDG104 and 09JDG001), Jiangsu University College Student Scientific Research Project (Y11A015), Postdoctoral Science Foundation of China (2012M511202), and Postdoctoral research Funding Schemes of Jiangsu Province (1102124C) for support.

References

- Xiao J, Liu BY, Wei G, Huang XC (2011) *Inorg Chem* 50:11032–11038
- Wang CY, Wilseck ZM, LaDuca RL (2011) *Inorg Chem* 50:8997–9003
- Du M, Wang XG, Zhang ZH, Tang LF, Zhao XJ (2006) *Cryst Eng Comm* 8:788–793
- Du M, Jiang XJ, Zhao XJ (2007) *Inorg Chem* 46:3984–3995
- Lu LH, Eychmuller A (2008) *Acc Chem Res* 41:244–253
- Kanegawa S, Karasawa S, Maeyama M, Nakano M, Koga N (2008) *J Am Chem Soc* 130:3079–3094
- Dybtsev DN, Chun H, Kim K (2004) *Angew Chem Int Ed* 43:5033–5036
- Liu PP, Cheng AL, Yue Q, Liu N, Sun WW, Gao EQ (2008) *Cryst Growth Des* 8:1668–1674
- Hu TL, Zou RQ, Li JR, Bu XH (2008) *Dalton Trans* 1302–1311
- Hartshorn CM, Steel PJ (1997) *Chem Commun* 541–542
- Sun WY, Fan J, Okamura T, Xie J, Yu KB, Ueyama N (2001) *Chem Eur J* 7:2557–2562

12. Shuichi H, Tao Y, Motoo S, Mitsuhiko S (2002) *J Am Chem Soc* 124:14510–14511
13. Shuichi H, Kaori H, Mitsuhiko S (2004) *Angew Chem Int Ed* 43:3814–3818
14. Liu HK, Sun WY, Ma DJ, Yu KB, Tang WX (2000) *Chem Commun* 591–592
15. Yin XJ, Zhou XH, Gu ZG, Zuo JL, You XZ (2009) *Inorg Chem Comm* 12:548–551
16. Gong Y, Li J, Qin JB, Wu T, Cao R, Li JH (2011) *Cryst Growth Des* 11:1662–1674
17. Lin JD, Long XF, Lin P, Du SW (2010) *Cryst Growth Des* 10:146–157
18. Wen LL, Lu ZD, Lin JG, Tian ZF, Zhu HZ, Meng QJ (2007) *Cryst Growth Des* 7:93–99
19. Zhu QL, Sheng TL, Fu RB, Hu SM, Chen JS, Xiang SC, Shen CJ, Wu XT (2009) *Cryst Growth Des* 9:5128–5134
20. Wang XJ, Liu YH, Xu CY, Guo QQ, Hou HW, Fan YT (2012) *Cryst Growth Des* 12:2435–2444
21. Lv DY, Gao ZQ, Gu JZ, Ren R, Dou W (2011) *Trans Met Chem* 36:313–318
22. Niu CY, Zheng XF, Wan XS, Kou CH (2011) *Cryst Growth Des* 11:2874–2888
23. Palmans ARA, Vekemans JAJM, Meijer EW, Palmans ARA, Kooijman H, Spek AL (1997) *Chem Commun* 2247–2248
24. Sheldrick GM (2008) *Acta Crystallogr Sect A: Found Crystallogr* 64:112–122
25. Ma LF, Wang LY, Hu JL, Wang YY, Yang GP (2009) *Cryst Growth Des* 9:5334–5342
26. Gu JZ, Gao ZQ, Tang Y (2012) *Cryst Growth Des* 12:3312–3323
27. Mu YJ, Han G, Li Z, Liu XT, Hou HW, Fan YT (2012) *Cryst Growth Des* 12:1193–1200
28. Ohkoshi S, Tokoro H, Hozumi T, Zhang Y, Hashimoto K, Bord I, Rombaut G, Verelst M, Moulin CC, Villain F (2006) *J Am Chem Soc* 128:270–277
29. Zheng XJ, Jin LP, Gao S, Lu SZ (2005) *New J Chem* 29:798–804